Large scale sand liquefaction flow slide tests revisited

M.B. de Groot, J. Lindenberg, D.R. Mastbergen and G.A. van den Ham
Deltares, the Netherlands

Abstract: Massive failure of submerged slopes form a major threat for many dikes along estuaries in the Netherlands, the subsoil of which consists of alternating layers of loosely packed and more densely packed sand. Static liquefaction in the loosely packed sand plays an important role. Insufficient knowledge is available to predict the flow of sand and the retrogression of the instability after initial liquefaction. Liquefaction flow slides have been studied during an extensive experimental research program in the period 1973 - 1977 on behalf of the design of the storm surge barrier in the Oosterschelde estuary. Results of this program are revisited to learn about the response of a loosely packed sand layer to a local instability. The program included more than a hundred of tests in a large and medium sized flume that were filled with sand. Each sand body had a horizontal surface and a slope as boundaries. A remarkable difference was observed between the tests in which retrogressive liquefaction flow slides did and those where such slides did not occur. This may be quite relevant for the understanding of flow slides in natural slopes with pockets of loosely packed sand. The test set-up, measurements and main results of the large scale tests are described in this paper.

Keywords: static liquefaction of sand, flow slide, large scale tests

1 INTRODUCTION

Hundreds of massive failures in submerged slopes occurred in the past century along the banks of estuaries in the Netherlands (Koppejan et al 1948; Silvis et al 1995). Massive slope failures are still a major threat for many dikes along such banks. The massive extent is probably related to a process in which a local instability caused by erosion or otherwise is followed by retrogression of the instability over a large distance, whereas the dislodged sand flows down along the slope. Dredging research (Van Rhee and Bezuijen 1998) and experience with occasional massive slope failures during dredging (De Jager et al 2008) provided knowledge about retrogression of breaches in more densely packed sand. This knowledge appears to be applicable to massive slope failures in nature as well (Mastbergen and Van den Berg 2003).

The subsoil in these estuaries, however, consists of alternating layers of loosely packed sand and more densely packed sand. Static liquefaction in the loosely packed layers contributes significantly to the cause and the extent of the slope failures. Methods for prediction of the initiation of static liquefaction are meanwhile rather well developed (Jefferies and Been 2006). However, prediction of the subsequent flow of sand and retrogression of the instability requires more insight in the response of a layer of loosely packed sand to a local instability (Figure 1).

Liquefaction flow slides in loosely packed sand haves been studied during an extensive experimental research program performed on behalf of the design of the large storm surge barrier in the mouth of the Oosterschelde estuary in the period 1973-1977. During the design it was reckoned that flow slides could endanger the stability of the barrier in view of the deep scour holes expected to grow adjacent to the bed protections at both sea and estuary side. An extensive experimental research program was performed to decide about the length of the bed protection and on potential measures like compaction of the loosely packed sand (Kroezen et al 1982). The research was performed by a team of hydraulic and geotechnical experts from Rijkswaterstaat and (predecessors of) Deltares.

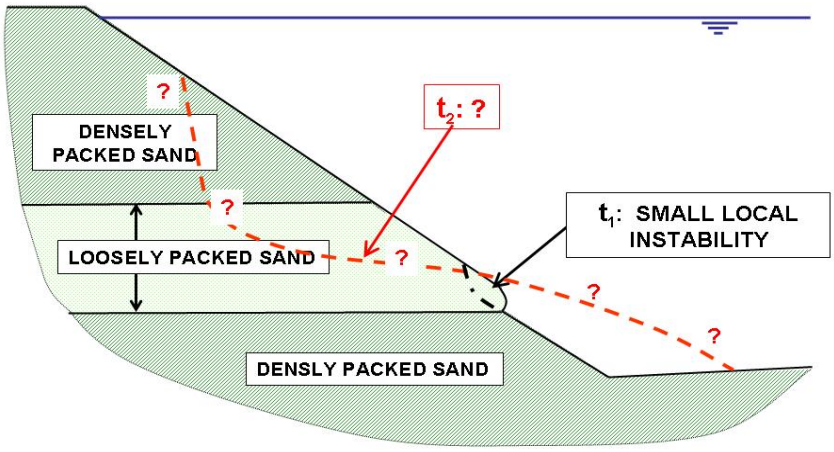

Figure 1 Question about response of loose sand to small local instability

The program included many tests in a large flume, both with and without a full scale bed protection mattress on top of the sand surface. It also included a large number of tests in a medium size flume. Several types of sand were used, the characteristics of which were extensively tested in the laboratory. Further variations included the density of the sand and the way the flow slides were initiated. Flow slides occurred in about half of the tests. In the other tests only small instabilities were observed. The development of pore pressures, level of the sand surface and sometimes the sand deformation were measured.

Conclusions about the relative density critical for flow slides and about the role of the bed protection helped the final design of the barrier. The barrier was completed in 1986. Since then several flow slides indeed occurred near the edge of the bed protection (De Groot and Mastbergen 2006), but no damage to bed protection or barrier was observed until now.

The tested loosely packed sand bodies, could be considered as models of loosely packed sand layers in a slope. Consequently, revisiting these tests may be a valuable tool to learn more about the response of a loosely packed sand layer to a local instability. The test set-up, the measurements and the most relevant results of the tests without bed protection will be presented in this paper, followed by a tentative explanation of the relevant physical phenomena.

2 DESCRIPTION OF EXPERIMENTAL PROGRAM

2.1 Survey of experimental program

The experimental program included two years of nearly continuous testing in the large flume, followed by nearly a year of testing in the medium size flume. The number of tests in the large flume was 38, the number in the medium size flume 95.

The first 13 large scale tests were used to develop a satisfactory test set-up. The subsequent 13 tests (nrs 14 – 26) were used to study the general behaviour of the sand either in loosely packed or in very loosely packed state and the role of a bed protection. The final series of 12 large scale tests (OS1 – OS12) focused on the determination of the value of the relative density critical for the occurrence of a flow slide as a function of grain size distribution and sand body height.

Most of the tests in the medium size flume focused on test set-up or instrumentation in view of future research (which ultimately was not performed). However, approximately 25 tests focused on the behaviour of the sand, such as scale effects and the influence of a significant reduction in grain size.

The program was performed more than 35 years ago. Many of its results have been carefully reported (in Dutch language). These enabled the authors, one of which himself was intensively involved in the experiments, to get a clear picture of the tests in spite of the many years past. Nevertheless not all relevant information could be recovered.

2.2 Test set-up in large scale flume

A 60m long part of a 3m wide and 3m high concrete flume with some glass windows in one of the walls was available for the large scale tests. See Figure 2. A gate of steel was constructed half way the flume in such a way that it could be lifted out of the flume by rotation. In closed position its slope was 2 (vertical) to 1 (horizontal). A 30m long sand body was placed behind the gate after the flume had been filled with water. Over a length of 24 m the sand was fluidised by means of a fluidisation device in the bottom of the flume in order to improve saturation and to create a low, desired density. The level of the sand surface varied per test at 1.3m, 2.3m or 2.4m above the flume bottom, i.e. 1.0m, 2.0m or 2.1m above the fluidisation device.

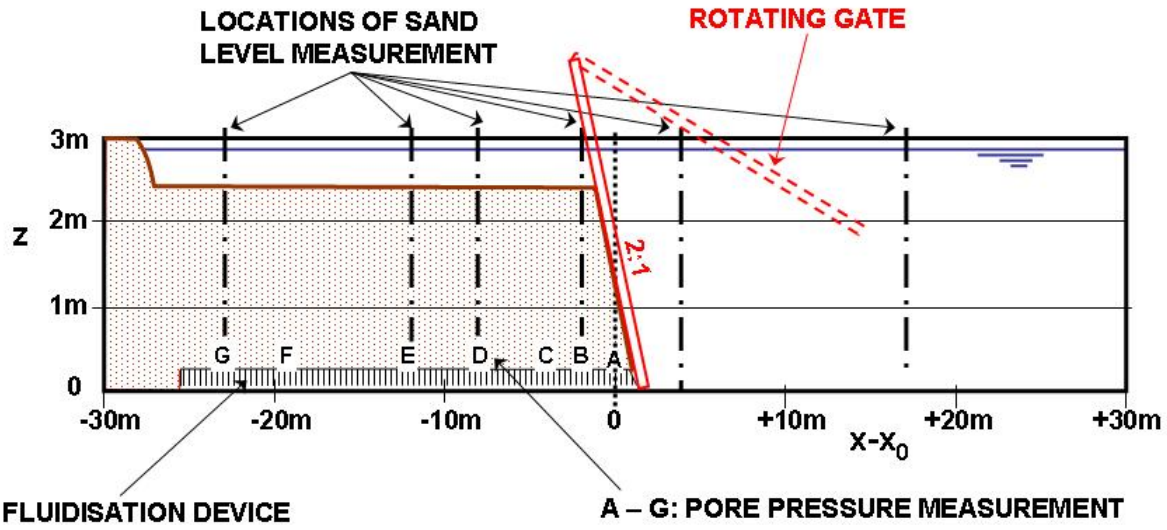

Figure 2 Test set-up in large flume

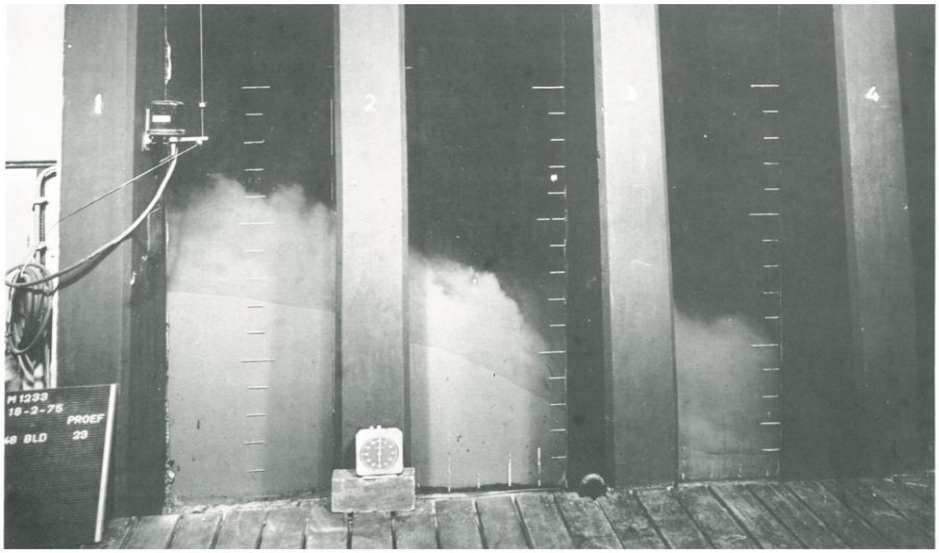

Figure 3 Picture of settled and flowing sand through glass windows at x –x0 ≈ 5m. Distance between white dashes 0.1m.

Instability was initiated at each test by lifting the gate with a velocity of approximately 0,1m/s. Then, the sand body behind the slope started to respond to its instable situation, a response that took several minutes after which the sand body found a new stable situation. A remarkable difference was found between tests resulting in flow slides and those which did not. The response was registrated in several ways:

- The sand surface was measured continuously at six locations by means of a slightly adapted wave height recorder, an instrument that registrates water level fluctuations – here sand surface fluctuations - by measuring electric resistance between two thin vertical metal strips.
- The flow of sand and the change in sand surface was observed through the glass windows and registrated by means of photography and video. See Figure 3.
- The whole sand surface was sounded in detail after it came to rest.
- Pore pressures were registrated at several places just above the fluidisation device and during some tests also at higher levels, along the walls.

2.3 Preparation of sand body in large scale flume

The fluidisation device was adapted several times, in the first place because it appeared quite difficult to create such a loosely packed sand bed that a flow slide could be initiated. Other problems were, among others, local variation of fluidisation water discharge through the bed, poor fluidisation near the walls, local variation of sand density.

The final fluidisation device consisted of 0.05m diameter PVC tubes with a large number of small holes at a distance of 0.25m at the bottom of the flume. The tubes were wrapped in geotextile to avoid clogging of the tubes. Their main direction was perpendicular to the walls, but they had a small slope with respect to the horizontal bottom of the flume. Each time fluidisation was needed during approximately one hour. The water was treated to prevent clogging of the small tube holes and to find constant values of the electric resistance of the water, relevant for the measurement of the sand density.

Fluidisation helped to remove the air out of the pores. But its main purpose was to create a homogeneous sand bed with sufficiently low density. Variation of the fluidisation discharge appeared to be a good way to manage the relative density of the sand bed in the range of interest between $0 < I_D < 0.3$. The higher the discharge, the lower the density.

A problem appeared to be the so called ‘pre-liquefaction’: local liquefaction starting immediately after the end of the fluidisation and resulting in local I_D values which were up to 0.15 higher than elsewhere. It occurred especially close to the gate, probably by shear strain related to the friction between the sand during its resedimentation and the relatively stiff gate. The occurrence of pre-liquefaction elsewhere could only be explained by (small) local variations in the fluidisation and resedimentation processes. To reduce the effect, fluidisation was often repeated several times until the measured excess pore pressures due to pre-liquefaction were sufficiently small to start the flow slide test.

2.4 Measurement of density in large scale flume

The density was measured by means of the in situ electrical resistivity probes, i.e. common CPT’s with electrodes at different heights. Four electrodes are used simultaneously: two to send an electric current with known strength through the sand and two to measure the voltage (Van den Berg, 1987). The distance between the two outer electrodes was either 0.5m (“combination A”) or 0.1m (“combination B”). The system was calibrated for each type of sand. An extensive program of testing and adapting the characteristics of the measurement system had been performed during the first 10 large scale tests. Placing of the probes in the sand before fluidisation had appeared to give too much disturbance of the local fluidisation. Consequently, the probes were brought in after fluidisation, although it often caused local liquefaction and densification. The local densification caused systematically higher densities ($\Delta I_D \approx +0.2$) found with combination B than with combination A. The values found with combination A are assumed the more reliable. The values of combination B, however, were used to check the disturbance of bottom, walls and sand surface on the homogeneity. In agreement with the very loose state derived from the electric resistivity, the cone resistance was extremely low in most tests.

At some tests the local densification caused by the probes was removed by repeating the fluidisation at the same discharge. Otherwise, the density was only measured at locations far from the gate before the test and in the undisturbed sand after the test, for as far a flow slide had not disturbed the whole sand body. At a few tests resulting in a large flow slide the density was measured also in the sand that had shown liquefaction and some deformation. No significant differences have been found between the densities before and after the flow slide.

Variations in relative density in vertical direction, as observed over the height of one probe, can be expressed by a typical standard deviation of $\sigma(I_D) = 0.03$; variations in horizontal direction by $\sigma(I_D) = 0.05$, if the locally higher values by pre-liquefaction and the region close to the gate are not taken into account.

2.5 Test set-up in medium scale flume

A 30m long part of a 0.7m wide and 1m high concrete flume with glass windows in one of the walls was available for the medium scale tests. A 5m to 5.4m long sand body was placed at one end of the flume during tests with coarse sand. For tests with fine sand the soil body was extended to 10m. A fluidisation device was present over the full length of the sand bodies. The sand surface was at 0.8m above the flume bottom, i.e. 0.63m above the fluidisation device. The test set-up was similar to that in the large scale test. A remarkable difference is the absence of the rotating gate in most of the tests. The steep slope was created by first bringing more sand in the flume and subsequently dredging some sand away until the desired very steep slope. This very steep slope (usually again 2:1) could be kept temporarily stable by suction of water through the fluidisation system. Initiation of instability was realised by stopping the suction of water.

The final sand surface was registrated in detail after completion of each test. During each test the drop of the sand surface was measured in small intervals in one vertical at 1.2m distance from the steep slope and registrated at video through the glass windows (not available any more). Pore pressures were measured in nearly the same vertical with pressure cells in the wall.

Special attention was paid to the registration of sand deformation and sand flow during several tests. The application of a sand flow velocity meter was unsuccessful. However, deformation or flow of the sand that did not move over more than approximately one meter was successfully done by colouring the sand with $KMnO_4$ in originally vertical "screens". Deformation could be observed during a test through the glass wall. The final displacement of sand, also at some distance from the wall, was observed by carefully digging the sand after the test.

3 SURVEY OF MAIN TEST RESULTS

3.1 Basic results

The tests in the large flume could be divided in three groups, depending on the observed results:
- Tests resulting in a flow slide; liquefaction was observed in all these tests
- Tests not resulting in liquefaction or flow slide
- Tests resulting in liquefaction, but not in a flow slide

All relevant tests in the medium scale flume resulted in flow slides.

Table 1. Survey of main results of tests in large scale flume resulting in flow slide.

Testnr	D_{50} [μm]	e [-]	I_D [-]	h [m]	$x_0 - x_{RGR}$ [m]	$x_{TOE} - x_0$ [m]	Δz [m]	V [m^3/m]	T_{RGR} [s]	dz/dt [m/s]	cot β [-]	u_{MAX} [kPa]	$t(u_{MAX})$ [s]	T_u [s]
14	145	0.835	+0.15	2.1	25	14	0.25	7	-			8	25	130
16	145	0.880	+0.02	2.1	25	32	0.87	19	56			11	8	150
17	145	0.905	-0.05	2.1	24	24	0.50	15	62			9.5	8	165
19	145	0.887	0.00	2.1	25	28	0.65	18	70	0.070	5.9	10	20	200
20	145	0.887	0.00	2.1	25	33	0.80	21	70	0.083	4.8	10	8	190
26	145	0.887	0.00	2.1	25	28	0.82	18	90	0.040	8.5	12	20	220
OS1	145	0.905	-0.05	2.0	23	32	0.90	17	-			13	13	150
OS7	145	0.905	-0.05	1.0	13	17	0.35	4	-			8.5	4	100
OS10	175	0.852	+0.02	2.0	23	44	0.95	23	-			8.5	20	110

Table 2. Survey of main results of tests in large scale flume not resulting in liquefaction or flow slide.

Testnr	D_{50} [μm]	e [-]	I_D [-]	h [m]	Lique-faction?	$x_0 - x_{RGR}$ [m]	$x_{TOE} - x_0$ [m]	V [m^2]	u_{MAX} [kPa]	$t(u_{MAX})$ [s]	T_u [s]
OS2	145	0,852	+0,10	2,0	yes	8	4	1.0	2.0	85	120
OS3	145	0.802	+0.25	2.0	no	3	3	0.8	-	-	-
OS4	145	0.835	+0.15	2.0	no	13	5	1.5	-	-	-
OS5	145	0.905	-0.05	1.0	yes	4	4	0.5	3.0	5	20
OS6	145	0.869	+0.05	1.0	yes	2	3	0.3	-	-	-
OS8	145	0.869	+0.05	1.0	yes	7	4	0.8	1.2	30	70
OS9	175	0.802	+0.17	2.0	yes	5	5	0.9	3.3	20	50
OS11	175	0.802	+0.17	2.0	no	3	5	0.8	-	-	-
OS12	175	0.845	+0.04	2.0	yes	3	5	1.0	6.0	20	120

Table 3. Survey of main results of tests in large scale flume resulting in liquefaction without flow slide.

Testnr	D_{50} [μm]	e [-]	I_D [-]	h [m]	Lique-faction?	$x_0 - x_{RGR}$ [m]	$x_{TOE} - x_0$ [m]	V [m^2]	u_{MAX} [kPa]	$t(u_{MAX})$ [s]	T_u [s]
OS2	145	0,852	+0,10	2,0	yes	8	4	1.0	2.0	85	120
OS3	145	0.802	+0.25	2.0	no	3	3	0.8	-	-	-
OS4	145	0.835	+0.15	2.0	no	13	5	1.5	-	-	-
OS5	145	0.905	-0.05	1.0	yes	4	4	0.5	3.0	5	20
OS6	145	0.869	+0.05	1.0	yes	2	3	0.3	-	-	-
OS8	145	0.869	+0.05	1.0	yes	7	4	0.8	1.2	30	70
OS9	175	0.802	+0.17	2.0	yes	5	5	0.9	3.3	20	50
OS11	175	0.802	+0.17	2.0	no	3	5	0.8	-	-	-
OS12	175	0.845	+0.04	2.0	yes	3	5	1.0	6.0	20	120

Table 4. Survey of main results of tests in medium scale flume resulting in liquefaction and flow.

Testnr	D_{50} [μm]	I_D [-]	h [m]	$x_0 - x_{RGR}$ [m]	$x_{TOE} - x_0$ [m]	Δz [m]	V [m^2]	T_{RGR} [s]	dz/dt [m/s]	cot β [-]	u_{MAX} [kPa]	$t(u_{MAX})$ [s]	T_u [s]
T28	200	0.00	0.6	5.4	4.7	0.13	0.85				3.0	13	37
T30	200	0.00	0.6	5.0	4.6	0.11	0.68				1.8	7	30
T31	200	0.00	0.6	5.2	5.0	0.09	0.80				2.7	10	33
T49	200	0.00	0.6										
T50	200	0.00	0.6										
T51	200	0.00	0.6										
T61	200	0.00	0.6	3.5	3.1	0.10	0.39		0.07	3.3	1.7	5	23
T72	200	0.00	0.6	4.0	4.7	0.15	0.60		0.11	2.7	1.1	3	20
T73	200	0.00	0.6	4.0	3.9	0.14	0.56		0.08	3.0	1.3	4	25
T75	200	0.00	0.6	4.2	3.9	0.13	0.54		0.09	2.1	1.4	3	33
T76	200	0.00	0.6	4.0	3.8	0.15	0.52		0.07	2.9	1.3	2	30
T77	200	0.00	0.6	4.1	4.3	0.15	0.60		0.07	2.7	1.5	3	33
T78	200	0.00	0.6	4.5	3.7	0.11	0.60		0.08	2.8	1.7	3	30
T79	200	0,00	0.6	3.6	3.4	0.12	0.50		0.05	3.6	1.8	4	30
T80	200	+0.04	0.6	3.0	2.4	0.12	0.32		0.08	2.8	1.3	4	20
T81	200	+0.06	0.6	2.0	2.0	0.11	0.26				1.2	2	15
T82	200	+0.04	0.6	1.5	2.2	0.12	0.26				1.1	2	13
T83	200	+0.04	0.6	3.0	2.9	0.13	0.41		0.06	2.5	1.9	3	30
T85	200	0.00	0.6	2.8	2.7	0.10	0.36		0.04	5.3	0.8	3	20
T86	200	0.00	0.6	4.5	3.8	0.07	0.48		0.02	11.3	1.9	3	30
T87	200	0.00	0.6	3.2	2.5	0.10	0.30		0.11				
T95	90	0.00	0.6	10	9	0.10	1.4	80	0.08		1.1		

The tests resulting in a flow slide distinguished from the other tests in a very remarkable way. All flow slides showed high excess pore pressures and retrogression of a negative sand wave over the horizontal surface. Basic results, like the final regression distance, x_0 - x_{RGR}, the final surface drop, Δz, the regression duration, T_{RGR}, the peak value of the excess pore pressure, u_{MAX}, and the total duration of excess pore pressure, T_u, are presented in the tables 1 to 4. See also list of symbols.

4 SAND PROPERTIES AND INFLUENCE OF DENSITY

4.1 Sand properties in large scale tests

First 34 tests were done with "Haringvliet Sand"; the last with "Oosterschelde Sand". The grains of both can be characterized as sub-rounded or sub-angular. Several sand samples were taken out of the large flume after the sand had been used during the first 26 tests and before the last 12 tests. Some Oosterschelkde Sand samples were taken out of the flume after last tests. The main results are presented in table 5. Earlier tests done on both types of sand had shown nearly the same values. Frequent fluidisation apparently did not influence its properties significantly.

Table 5. Characteristics of sands used in large scale tests

Sand type	D_{50} [μm]	D_{10} [μm]	D_{60}/D_{10} [-]	Percentage D<16μm [%]	e_{MIN} [-]	e_{MAX} [-]	$e_{CRIT,DRY}$ [-] (σ_c in kPa)	$e_{CRIT,WET}$ [-] (σ_c in kPa)
Haringvliet	145 ±5	100 ± 5	1.60 ± 0.05	3 ± 1	0.550 ± 0.012	0.887 ± 0.020	> 0.79 (10kPa) 0.78 (20kPa) 0.75 (40kPa) 0.72 (60kPa)	0.812 (10kPa) 0.802 (20kPa) 0.786 (50kPa)
Oosterschelde	175 ±10	115 ± 5	1.65 ± 0.07	2 ± 1	0.520 *) ± 0.015	0.859 ± 0.020	> 0.77 (10kPa) 0.75 (20kPa) 0.70 (30kPa) 0.68 (50kPa)	0.776 (10kPa) 0.764 (20kPa) 0.757 (50kPa)

*) One of the tests gave e_{MIN} = 0.590. There are reasons to assume that the outcome of this test was wrong.

The dry critical void ratio, $e_{CRIT,DRY}$, is the lowest void ratio at which contraction occurs when a dry sample is sheared in a triaxial cell after isotropic consolidation to σ_c and maintaining σ_c constant during shearing. The wet critical void ratio, $e_{CRIT,WET}$, is the lowest void ratio at which just meta-stability (or "instability") occurs when a saturated sample is sheared undrained in a triaxial cell after isotropic consolidation to σ_c. Details of the procedure are explained by Lindenberg and Koning (1981).

It was not common in the seventies to determine the critical state or the steady state when testing sand. The wet critical density tests, however, are the same tests used to find the critical state. The critical state can be estimated by assuming the mean effective stress, p', at the wet critical void ratio to be equal to one fifth of the consolidation stress. Wet critical density and the approximate critical state lines are indicated in Figures 4 and 5. The slope of the critical state line for Haringvliet Sand is λ_{10} = 0.05 and the void ratio of the critical state line at p'=1kPa, e_c(1kPa) = 0.832, which means that e_{MAX}- e_c(1kPa) = 0.055. The corresponding values for Oosterschelde Sand are λ_{10} = 0.04 and e_c(1kPa) = 0.788, which means that e_{MAX} - e_c(1kPa) = 0.071. These values are quite common for uniform sand with a small fines content at low stress level, as follows from section 2.6 of Jefferies and Been (2006).

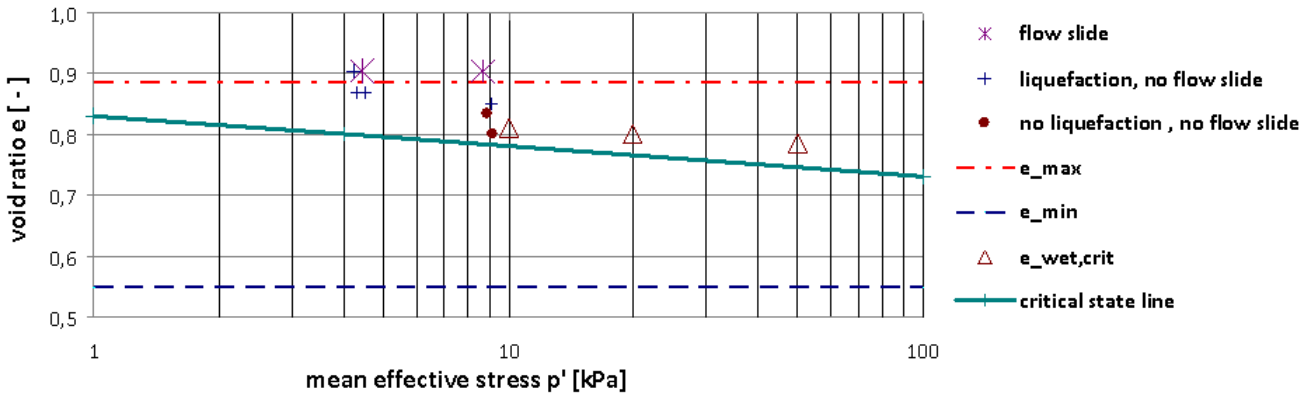

Figure 4 Sand characteristics and void ratios in 8 large scale tests on Haringvliet Sand

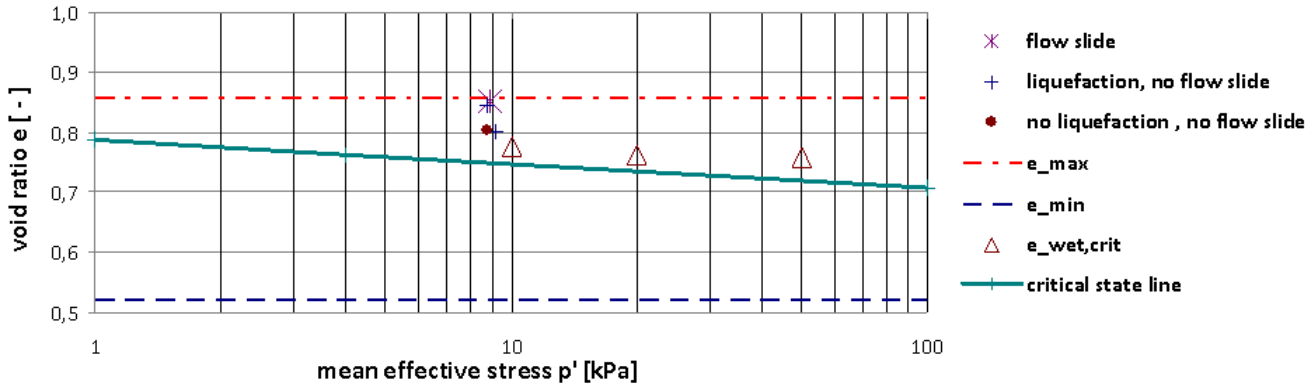

Figure 5 Sand characteristics and void ratios in 4 large scale tests on Oosterschelde Sand

4.2 Relative density critical for liquefaction and flow slide

The 12 large scale tests OS1 – OS12 were specially designed to study the role of the relative density. The outcome is presented in the Figures 4 and 5, were the value of the mean effective stress is assumed to be p'=h/2x(1-n)x16.5kN/m^3. Liquefaction only occurs if the relative density is very low. A flow slide requires an even lower value, although the difference between both conditions is hardly significant. The condition for a flow slide can be expressed in terms of a density index (taking into account the low stress level) or the so-called state parameter, being the distance of the present void ratio from the critical state line (at the same value of p') in figure 4 and 5:

- $I_D \leq 0.0 \pm 0.1$ at this low stress level
- $\psi \geq 0{,}10 \pm 0.05$.

4.3 Sand properties in medium scale tests

Two types of sand were used, some of which' characteristics are presented in table 6. Most likely both sands were sub-angular to sub-rounded. The density of the sand was the lowest that can be realised by the fluidisation for nearly all tests. The values of the density index, I_D, are not reported, but are likely to be close to I_D=0. During tests T80, T81, T82 and T83 slightly higher values were used.

Table 6 . Characteristics of sands used in medium scale tests

Sand type	D_{50} [µm]	D_{60}/D_{10} [-]	Percentage D<16µm [%]
Coarse	200	1.4	< 3
Fine	95	1.5	< 5

5 DETAILED RESULTS OF TYPICAL TESTS

5.1 Test in large flume resulting in flow slide

Test number 20 is a typical example of the tests in the large flume with very loosely packed sand resulting in a flow slide. Its results are summarized in the figures 6 to 11. The flow slide started immediately after turning away of the gate.

Figure 6 shows the sand surface development. A “negative sand wave” progressed to the left (“retrogression”) with high speed, whereas sand flowed out to the right of the gate resulting in an ever more gentle slope with a toe progressing to the right with a similar high velocity. After approximately one minute the negative sand wave reached the location where the fluidisation device ended (i.e. in the densely packed sand). Not much later (t = 75s) the surface profile reached practically its final shape.

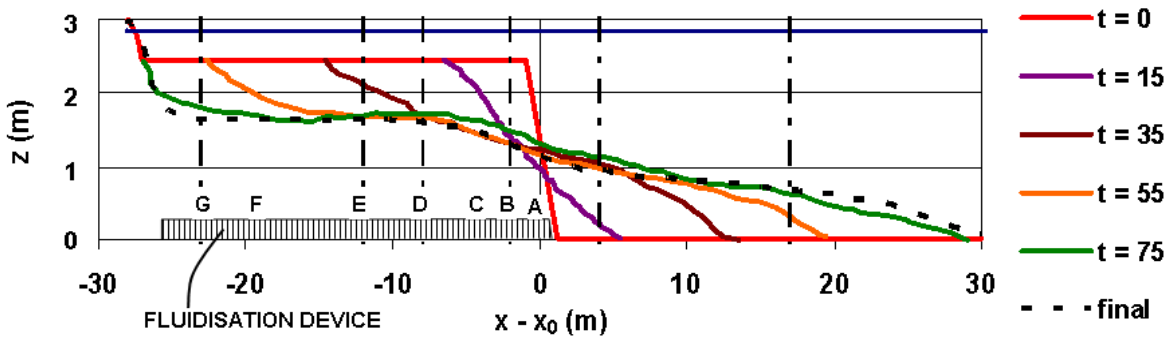

Figure 6 Sand profile development in test nr 20

The retrogression/progression velocities where quite constant, as illustrated in Figure 7. The front of the wave created a sharp change in surface slope from horizontal to slope with angle β (Figure 9). The front slope angle, can be derived at the locations of sand surface measurement by combining the surface height loss velocity at the moment of the passing front dz/dt with the retrogression velocity. The slopes at the locations B, D, E and G were, respectively, cotβ=3.8, cotβ=4.5, cotβ=4.5 and cotβ=9.2.

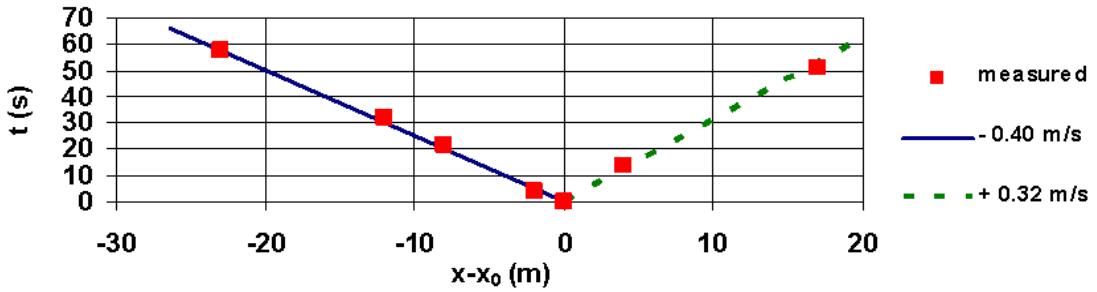

Figure 7 Regression of sand wave and progression of toe in test nr 20

Excess pore pressures u developed in the same period, as illustrated in Figure 8. The measured pore pressures at the flume bottom could be the result of complete liquefaction over a limited height or partial liquefaction over the full height or partial liquefaction over a limited height. Pore pressure measurements at higher levels during later similar tests did not confirm which of these assumptions is true. They made only clear that the excess pore pressures varied significantly in three dimensions and in time. The assumption of complete liquefaction over a limited height is worked out in Figure 9 for four moments representative for the retrogression period. It could be seen that the retrogression velocity of the liquefaction was approximately equal to that of the sand wave.

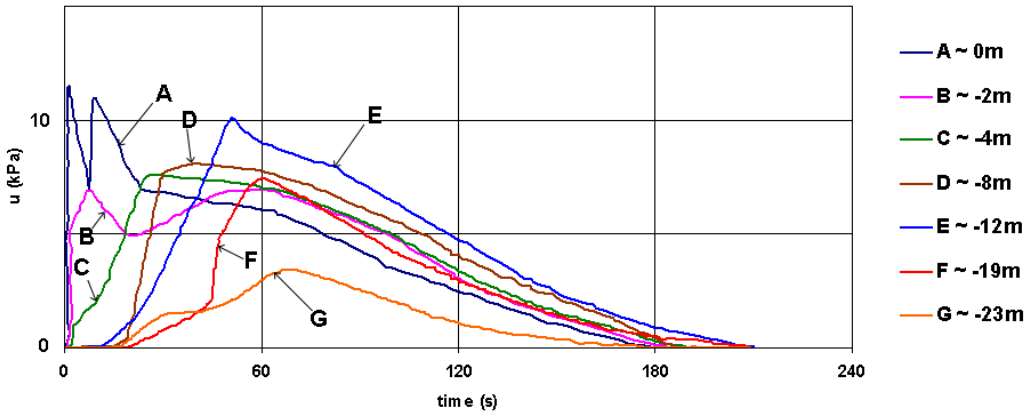

Figure 8 Development of excess pore pressures u in test nr 20

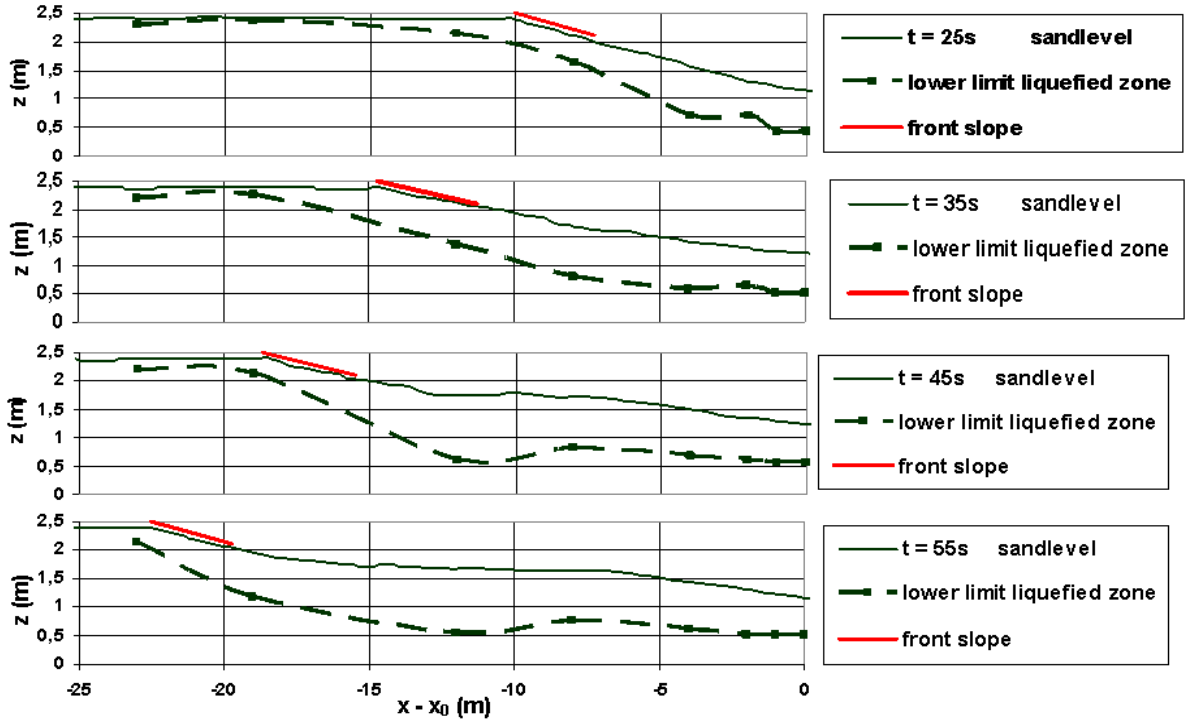

Figure 9 Subsequent sand profiles and thickness of liquefied zone in test nr 20

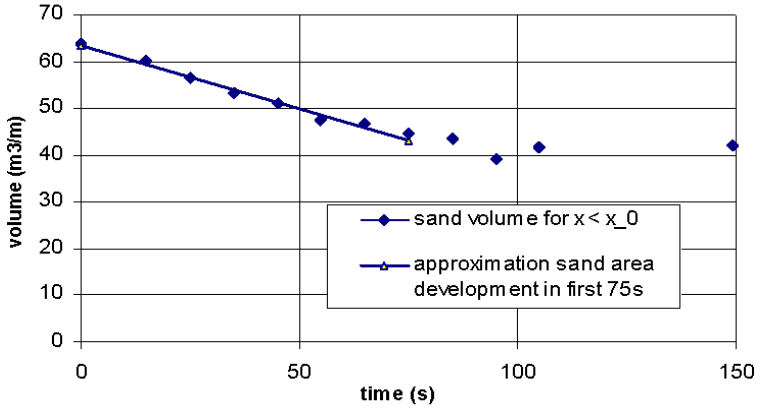

Figure 10 Development of sand volume per unit width for x < x0 in test nr 20

The volume of the sand body at the left-hand side of its original 2:1 boundary decreased at a nearly constant velocity during the retrogression of the sand wave, as illustrated in Figure 10. This velocity decreases at the end of the retrogression period $T_{RGR} \approx 75$s. No significant change in volume takes place after 100s, although pore pressures are still in excess of the hydrostatic pressure during another 80s (Figure 8). The volume of displaced sand per unit width can be derived from the first and the last point in Figure 10: V= (63 - 42) = 21m^3/m. The total volume was 3m.21m^3/m = 63 m^3.

The sand discharge can be derived from the change in sand volume with time for a moment half way the sand wave retrogression (Figure 11). According to visual observation, a small part of the discharge takes place as a turbulent cloud of water with some grains just above the sand surface and most of the discharge takes place by the quick movement of the upper centimeters of the sand body. Some slow shear deformation in the decimeters below this quickly moving sand may also contribute to the discharge, whereas the lower half of the sand body hardly moves at all.

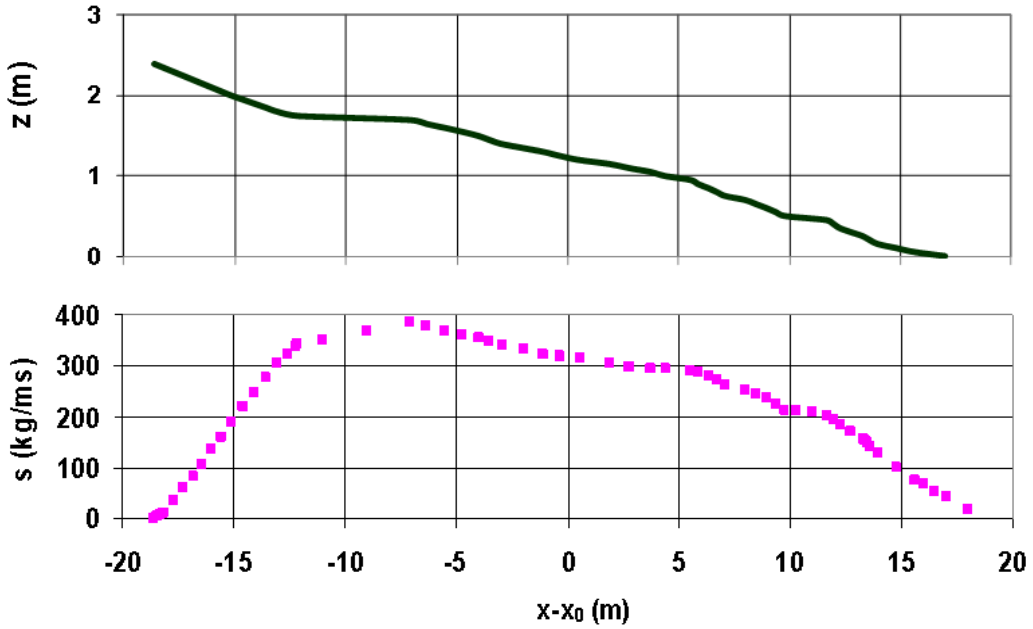

Figure 11 Sand discharge at t = 45s in test nr 20

5.2 Test in large flume not resulting in liquefaction or flow slide

Test OS3 may be considered to be representative for those large scale tests which did not result in a flow slide and also did not show any liquefaction. The density created at this test was relatively high ($I_D \approx 0.25$). The instability, initiated by turning away the gate, was just superficial: sand grains were detached one by one from the surface and rained down along the steep slope and created a new slope after sedimentation at the toe. No significant excess pore pressures were measured; just some under-pressures close to the original slope. This process continued for approximately 5 minutes, which is much longer than the flow slides in other tests and only slightly longer than the process in most other tests in which no flow slide occurred. The retrogression velocity was approximately 3m/300s=0.01m/s. This is approximately two or three times the retrogression velocity of a vertical breach in dilative sand according to (Mastbergen and Van den Berg 2003), which would be equal to $k.\{1/(e_{MAX}-e)\}.1{,}65/\tan 30°$.

The final result was a slope profile with a retrogression distance of 3m and an out-flow distance of 3m, thus $\cot\alpha=(3m+3m)/2=3$. The middle part of the slope was steeper: nearly the natural slope..

5.3 Test in large flume resulting in liquefaction without flow slide

The first response of the sand body in test OS5 to turning away the gate, was a wave-like movement of the horizontal surface over a length of several meters. This was observed through the glass windows. The upper layer with a thickness in the order of 0.1m looked like a completely liquefied mass. This sand started to move slowly in the direction of the original slope, which resulted in a settlement of the

horizontal surface of 0 to 0.1m and a slight blowing up of the original steep slope. After 20s the sand suddenly “froze”, after which only the steep slope showed instability similar to OS3: sand grains were raining down the slope. The final slope was similar to the one of OS3, with the exception of a gently sloping part where the sand had been liquefied.

At some locations excess pore pressures were measured during test OS5. These pressures were limited and did not continue over a long time. Higher excess pore pressures may have occurred at locations where no instruments were present.

5.4 Tests in medium scale flume resulting in flow slide

Flow slides occurred in all relevant tests in the medium size flume. Typical results of the tests were very similar to those in the large scale flume. The smaller height of the sand body resulted in smaller values of retrogression and outflow and lower excess pore pressures and, at least for the coarse sand. Less time was needed for the whole process. Special attention will be paid to test T95 and T50.

Test T95 was the only one with fine sand. Its profile development (Figure 12) shows that the drop of the sand surface was small, but the retrogression distance large. The retrogression took much more time than in the other medium scale tests with coarse sand.

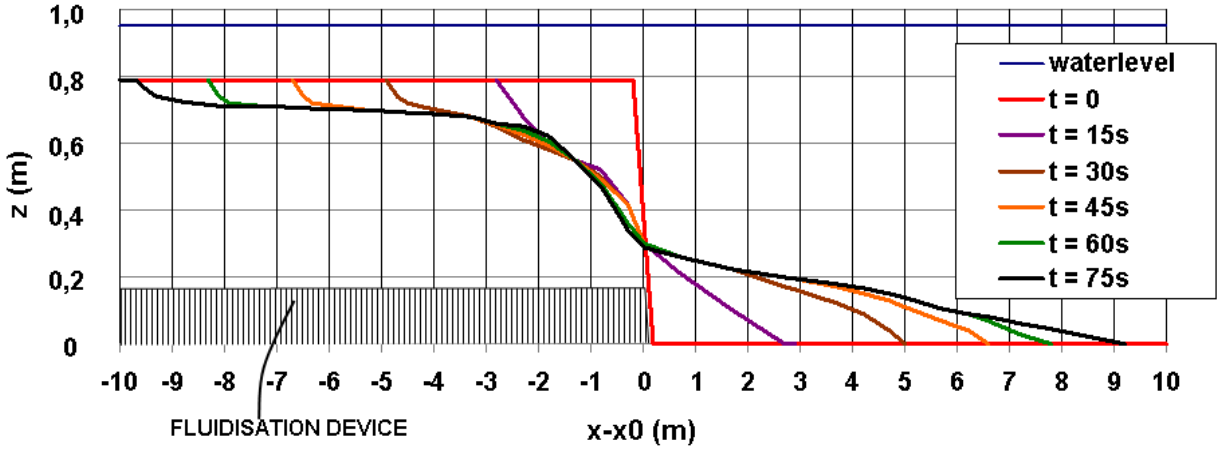

Figure 12 Sand profile development in test nr T95

Test T50 is one of the tests in which colour “screens” have been applied. The deformed screens observed along the glass wall at the end of the test are sketched in Figure 13. Unfortunately, the profile of the sand surface of this test once the flow had stopped was apparently not documented. The surface sketched in the figure is the one of test T73, which is reported to have nearly the same result as test T50. Approximately equally deformed colour screens have been found at several other tests.

If Figure 13 is representative for the mean results of the medium scale tests with D_{50}=0.200mm and $h_L \approx 0.2$m, it suggests that deformation occurs over the whole liquefied zone, but only very limited at the bottom of the liquefied column, where liquefaction ends very quickly. The largest horizontal distance traced by the coloured sand at $x\text{-}x_0$ = -0.9m is approximately $3h_L \approx 0.6$m. The volume of sand displaced through $x\text{-}x_0$ = -0.9m from the bottom to the top of the colour screen is approximately $0.2 \cdot h_L \cdot 3h_L = 0.6 \cdot h_L^2 = 0.024$ m^3/m. This is less than 10% of the total volume of displaced sand V(-0.9m) ≈ 0.4 m^3/m.

After flow stopped, the highest point of nearly each screen is situated a few centimeters below the final sand surface. The coloured sand grains originally present above this point must have been flowing away over a large distance, whereas some other grains coming from the left of the screen settled on top of the screen. Larger displacement of coloured grains (order factor 2) was found in the middle of the flume during carefully digging of the sand afterwards.

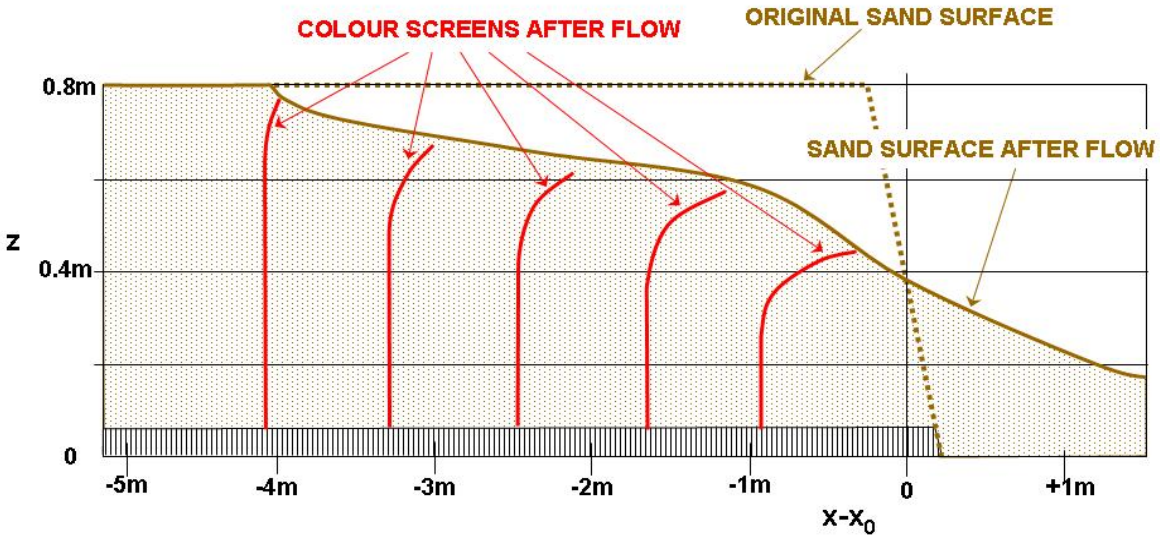

Figure 13 Deformation pattern along glass wall at medium scale tests with coarse sand

6 INTERPRETATION OF PHYSICS IN FLOW SLIDES

6.1 Main features of flow slides

The flow slides observed in test nr 20 and all other tests resulting in flow slides, have some remarkable characteristics:

- Sudden high excess pore pressures in the vicinity of the initial slope immediately after initiation of the instability.
- Retrogression of the high excess pore pressures at high speed. Excess pore pressures at any location rise quickly and decrease gradually at a constant speed which hardly varies from place to place.
- Retrogression of a negative sand wave at approximately the same high speed as the excess pore pressures and simultaneous progression of the toe resulting in a quite gentle final slope

A first global interpretation of the physics of these characteristics will be presented in this section. The three characteristics will be discussed subsequently, although the authors are convinced that there is a strong interaction between excess pore pressures, loss of instability, deformation of the grain skeleton and/or movement of sand grains at the surface with the consequent change in surface profile and change in stresses. The estimated values apply for test nr 20.

6.2 Sudden excess pore pressures near initial slope

The sudden excess pore pressures can be explained as the sudden liquefaction in undrained triaxial tests on loosely packed sand (Kramer and Seed 1988) The start of the test causes a sudden change in load in the sand body, which can only respond undrained. All sand elements follow the undrained stress path, the characteristics of which are a function of the relative density and original stresses. In case of loosely packed sand this path is characterised by a peak value for the shear stress (metastability point or instability point) due to contraction in shear (strain softening). The change in shear load of the sand elements close to the original slope exceeds this peak value which leads to instability of these sand elements, i.e. large shear deformation, increase in pore pressure and decrease in shear strength in a fraction of a second. This sudden strain softening of the sand elements close to the original slope yields an immediate increase in shear load of the elements at greater distance, some of which become instable as well.

6.3 Development of excess pore pressures during retrogression

6.3.1 Development of excess pore pressures in horizontal direction

The excess pore pressures in the points A and B (Figure 8) near the original slope rise in less than a second. The excess pore pressures in the points C, D, E and F at greater distance rise more gradually and arrive at their maximum values later, depending on the progress of the sand wave in negative x-direction ("retrogression"). The order of magnitude of the maximum in these points does not deviate from the ones in A and B. Which mechanism causes this retrogression of the excess pore pressures? Two potential mechanisms will be considered, traditional consolidation and contraction.

Consolidation process in case of constant total stress and the absence of any pore water source concerns the horizontal flow of water due to the horizontal component of the pressure head gradient in combination with storage of water in the pores due to decrease of mean effective stress. Indeed, the sudden excess pore pressure close to the original slope brings about such flow. The progress according to this mechanism can be described by the equation:

$$\partial u/\partial t = c_v \partial^2 u/\partial x^2$$

where $c_v = k(K+4/3G)/(\rho_w g)$ is the consolidation coefficient for unloading.

Last coefficient can be estimated from numerous tests on similar sands. Given the small grain diameter, the loose packing and the low stress level, the value can be estimated to be $c_v \approx 0.1$ m^2/s. The order of magnitude of the derivative of the pressure gradient can be estimated from the pore pressure measurements at one moment (compare Figure 9), yielding $\partial^2 u/\partial x^2 \approx u_{MAX}/(5m)^2$, at least during most of the retrogression period. Thus, $\partial u/\partial t \approx u_{MAX}/1000s$ is found. This estimate is very rough. The real value may be ten times as large or may be just a tenth. Nevertheless, the real values of $\partial u/\partial t$ are much larger having the order of magnitude of $u_{MAX}/20s$ (Figure 8). Apparently this mechanism does not significantly contribute to the retrogression of liquefaction.

The other mechanism is contraction, which works as a kind of negative storage and can be modelled as a positive source of pore water. Contraction is the same mechanism of the sudden increase in excess pore pressure near the initial slope. However, contraction only occurs if the shear load changes. Such changes occur at some distance from the original slope at the moment the sand wave passes. Then, the sloping surface causes a shear stress in horizontal direction, which is increased by the horizontal component of the pore pressure gradient. Rotation of the principal stresses may take place if a deviator stress is initially present due to difference between the normal effective stress in horizontal en vertical direction. Such rotation may cause contraction even if the deviator stress does not increase. Most likely these changes, although much less than close to the initial slope at the start of the instability, are sufficient to cause strain softening in many sand elements. These elements are loosely packed enough to liquefy (nearly) completely and become instable.

The size of the wave, which can be characterised by Δz, determines the depth to which sufficient shear load changes occur and, consequently, the thickness of the liquefaction zone, h_L.

6.3.2 Development of excess pore pressures in vertical direction

Thus, contraction and shear cause large excess pore pressures in many elements in one sand column when the sand wave passes. The consequent excess pore pressure gradient may have a horizontal component, as discussed above, but the main component is vertical: flow of water to the surface. Simultaneously, the grains, which have lost effective stress, find a new grain skeleton with higher density. Following the assumption that the measured pore pressures at the flume bottom are the result of complete liquefaction over a limited height, rather than partial liquefaction over the full height (Figure 9), it can be stated that a process of resedimentation takes place in which pore water is expelled due to the higher density. This process concentrates in a resedimentation front at the lower end of each column, whereas the rest of the column remains fluidised by the upwards flowing water. The front rises with a constant velocity, causing the liquefied column to decrease in height until the front reaches the surface and liquefaction ends.

This process is observed in many other tests. A quantitative description is presented in (Bezuijen and Mastbergen 1988). The decrease in porosity Δn at resedimentation can be calculated from their equations (2) and (5) as a function of the original column height h_L, the permeability of the sand k and the duration of the excess pore pressure $[T_U - t(u_{MAX})]$:

$$\Delta n = \{T_U - t(u_{MAX})\}.k.(\rho_s - \rho_w).(1-n)^2/(\rho_w.h_L)$$

These values have been calculated for all tests, resulting in $0.004 < \Delta n < 0.02$, which are values similar as found by Bezuijen and Mastbergen (1988).

The sedimentation process takes much longer than the time in which most deformation takes place ($T_u >> T_{RGR}$). Consequently, the deformation of the sand slope does not stop because the sedimentation is completed, but because there is insufficient driving force for further deformation, as will be discussed in section 7.8 and 7.9.

6.4 Retrogression of negative sand wave and flow of sand

6.4.1 Sand flow regimes

Retrogression of a negative sand wave means the flow of sand in the positive x-direction. The process of retrogression of the negative sand is quite constant, as can be seen in the Figures 6, 7, 9 and 10. Figure 9 makes also clear that the moment t=45s may be considered representative for a large part of the process in test 20. The development of the sand flow for this moment is illustrated in Figure 11. Three sand flow zones may be distinguished:

- A zone of strong increase in sand discharge, for $-18m < x-x_0 < -11m$
- A zone of slight decrease in discharge for $-11m < x-x_0 < +13m$
- A zone of strong decrease in discharge for $+13m < x-x_0 < +18m$

The discharges presented in Figure 11 are derived from the changes in sand volume, as found from the sand surface development. The distribution of the discharge in vertical direction is probably very uneven. In sub-section 6.4.3 it will be explained that a large part of the flow is most likely concentrated in a relatively thin layer, where the sand grains move completely dislodged from their original sand column.

6.4.2 Zone of strong increase in sand discharge

Dislodgement of sand grains dominate the first zone. A sand grain may be said to be dislodged as soon as it is no longer part of the sand skeleton and moves away from its former neighbour grains. What causes the difference between the grains in the thin layer and the other ones, whereas reduction to (near) zero of the effective stress occurs for all grains of the liquefied column?

A first difference concerns the shear load caused by the slope induced gravity component parallel to the surface. This load is relatively strong at the surface and reduces with depth. This is especially relevant in the front of the sand wave where the slope (β) is relatively steep.

A second difference becomes relevant at larger distance from the front: shear load caused by the sand grains, dislodged earlier and flowing over the surface help to dislodge sand grains out of the top of the column.

The question may be raised whether a slight increase in distance between the dislodged sand grain and its former neighbour grains is needed to enable dislodgement. If so, this requires some net inflow of water. May this water come from above by a kind of dilation or dispersive force among the grains as soon as they move parallel to the surface with a velocity that strongly increases in upwards direction?

No dislodgement takes place any more at the boundary with the second zone or all dislodgement is compensated by sedimentation of grains out of the mass of grains flowing over the surface. This may be due to the more gentle slope.

The flow of sand in the first zone is not only characterised by the dislodgement of grains, but also by acceleration of these grains. The velocity a grain reaches when it descends over Δz if only gravity would be active $v(grain) = \sqrt{\{2\Delta z.g.(1- \rho_w/\rho_s)\}}$. At $x-x_0 = -11m$ in test 20, the maximum value of Δz = 2.4m – 1.7m = 0.7m (Figure 9). Thus $v(grain) \leq 3.0$ m/s. It is not likely that any grain reaches this velocity, as also friction along the surface will act and friction with the surrounding water. Last effect will cause water to be accelerated as well, such that a mixture of sand grains and water will flow over

the surface rather than individual grains. Nevertheless the acceleration is large enough to have inertia play a significant role in the development of the sand flow.

6.4.3 Equilibrium sand flow in middle region

The second zone is characterised by a nearly constant sand discharge. This means a near equilibrium between sedimentation and dislodgement. As the slope is constant over a large distance (approximately 1:20 in test 20), also a near equilibrium between gravity and shear resistance is present and a nearly constant velocity with constant layer thickness may be assumed: equilibrium sand flow.

The discharge at t = 45s in test 20 is $q_s = 0.2 \pm 0.05$ m^3/ms or approximately s = 300 kg/ms. Like with test T50 (Figure 13; section 5.4) it is assumed that not more than 10% of the sand is transported by gradual deformation of the liquefied sand body and that at least 90% is flowing in a thin layer at the surface. The velocity of the grains at the top of the thin layer is likely much higher than the one at the boundary between sand skeleton and thin layer.

Visual observations reported about the flow in the thin layer mention laminar flow. This may be similar to the flow observed in other large scale tests (Bezuijen & Mastbergen 1988) where liquefaction flow slides took place in a slope of very loosely packed sand. Detailed video records are still available of those flows and make clear that the deformation of the sand body is very similar to the one presented in Figure 13: hardly any movement in most of the liquefied sand body and a strong increase in velocity more close to the surface with quickly, laminarly flowing sand in the upper few centimeters of the sand body. A more or less clear boundary is present between the grains that move quickly along the surface without upwards movement and a cloud of turbulent water with occasional grains. High velocity gradients are observed in the quickly, laminarly flowing sand. More research is needed to find out whether the flow can be considered to be a “macro-viscous” flow or a “grain-inertial” flow as discussed by (Bagnold 1954).

To get an impression of the velocities and the velocity gradients that might have been present, the following speculative estimates are made. If the thickness of the thin layer is 0.2m, the mean flow velocity is 0.9·0.2/0.2 = 0.9 m/s. If the velocity of the sand grains at the top of the thin layer are twice the mean velocities, then they flow with 1.8 m/s and the mean velocity gradient in vertical direction du/dz = 1.8/0.2 = 9/s.

From previous investigations it is known that the slope angle at which an equilibrium flow is reached decreases with sand discharge and increases with grain size. Some quantitative information will be presented in section 7.9.

Surprising is the absence of a remarkable change at $x=x_0$ or a few meters beyond this point, as high excess pore pressures are present upstream of this point (see locations A to D in Figure 8 at t=45s), whereas it is not likely that excess pore pressures are present downstream of this point. At least that is the region where most of the sand has been sedimented after having flown in the thin layer. The reported visual observations do only speak about sand movements at the top of this part of the sand and not of flow slides. Unfortunately no pore pressures have been measured for $x>x_0$. The slope for $x>x_0$ becomes slightly steeper, but only for $x>x_0 + 8$m.

6.4.4 Sedimentation in region with strong decrease in discharge

The decrease of discharge means much sedimentation. It mainly takes place at the lower part of the slope, resulting in the progress of the toe. The toe has a relative steep slope. This can be concluded from the series of 12 photographs taken during test 20 and from the measured sand level at $x-x_0=+17$m which rises from zero to 0.3m in 5s (corresponding to a slope of 1:5, given the progress velocity of 0.32m/s, Figure 7). This means that nearly all sedimentation occurs at this slope and not at the horizontal flume bottom. Apparently this slope is much more gentle than the equilibrium flow for the discharge remaining at the last meters and the shear is sufficient to decelerate the grains.

7 EXPECTED EFFECTS OF LENGTH SCALE AND GRAIN SIZE

7.1 General

Extrapolation of the results to other conditions requires knowledge of the effects of length scale and grain size. Comparison between the results of the large scale tests and the medium scale tests gives an impression of some length scale effects. Comparison between the results for different grain sizes gives an impression of the influence of the grain size. Both effects are discussed in this section. Tentative conclusions are formulated.

7.2 Relative thickness of liquefied zone h_L/h

The length scale of each test can be expressed by the height of the sand body, h, or by the thickness of the liquefied zone h_L, defined as $h_L = u_{MAX}/[(1-n)(\rho_s-\rho_w)g]$. Last parameter seems to be a more determining scaling parameter than the height of the sand body h.

Interesting is the influence of scale on the relative thickness of the liquefaction zone h_L/h for all tests resulting in flow slides. It varied between 0.5 and 0.95 (mean value $h_L/h = 0.6$) in the large scale tests and between 0.15 and 0.56 (mean value $h_L/h = 0.3$) in the medium scale tests (Figure 14). Thus, it looks like a smaller scale yields less relative liquefaction. It may be due to the increase in stress level and the consequent higher sensitivity to contraction and liquefaction for sand elements with the same relative density. That would mean that this type of liquefaction flow requires a minimum thickness of the loosely packed layer of 0.3m to 0.5m.

The grain size does not appear to have any influence.

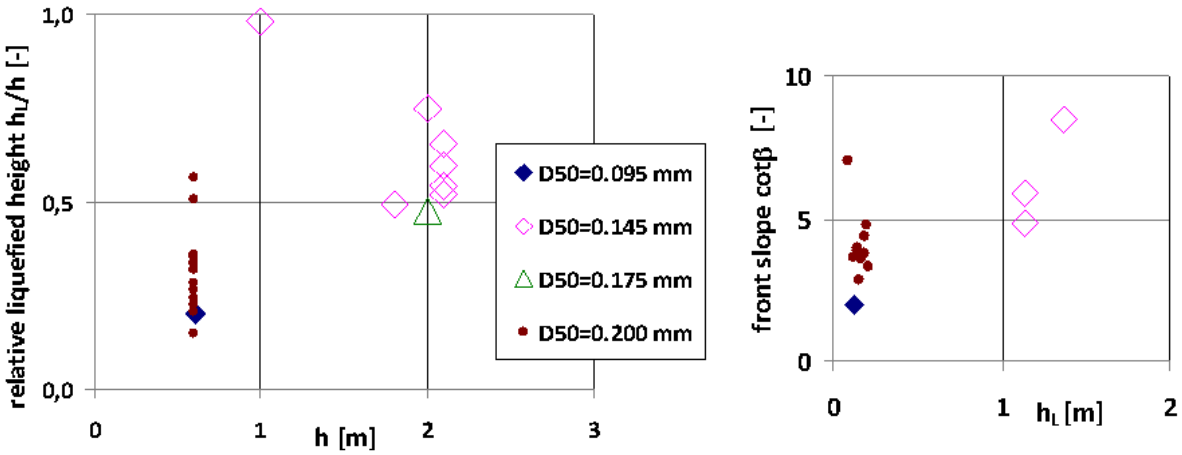

Figure 14 Liquefied height and front slope as function of length scale and grain size

7.3 Relative surface level drop $\Delta z/h_L$

The value of the relative drop of the surface level, $\Delta z/h_L$, varied between 0.3 and 1.2 with no significant influence of length scale or grain size.

7.4 Front slope β during retrogression

The sand surface during the flow slide can be characterised by front slope β. Its value varies during the retrogression of the sand wave. At first it is equal to the original slope, but more relevant is the more or less constant value that occurs in the middle of the retrogression period, e.g. $0.2T_{RGR} < t < 0.8\ T_{RGR}$. The values presented for the large scale tests (table 1 and Figure 14) are those observed in x_0-x=12m (vertical E of Figure 2) at $t \approx 0.5T_{RGR}$. The values presented for the medium scale tests (table 4 and Figure 14) are those observed in x_0-x=1.2m at $t \approx 0.3T_{RGR}$. The front slope is slightly more gentle with larger grain size and larger length scale. It is not clear whether this should be considered to be significant or not.

7.5 Velocity of excess pore pressure decrease

Figure 8 shows that the excess pore pressure, after having reached its peak, decreases gradually with a velocity that does not vary as much, neither in time, nor in place. This type of behaviour is observed in all tests. A characteristic descending velocity for each test can be defined by considering the value of $u_{MAX}/[T_U - t(u_{MAX})]$. This value varies between 0.05 and 0.13 kPa/s for all large and medium scale tests with the exception of the single test (T95) with very fine sand (D_{50} =95µm), where 0.008 kPa/s is found. The decrease corresponds most likely to the "resedimentation" process described in section 6.3.2. Its velocity is proportional to the permeability, k, which is a strong function of grain size. This is confirmed by the observations.

7.6 Retrogression velocity c

The retrogression velocity c (Figure 7) is not measured in each test, but its value can be estimated as $c = (x_0 - x_{RGR})(T_U/2)$. The velocity varies between relatively narrow boundaries: $0.25m/s < c < 0.45m/s$, with the exception of the single test with very fine sand (T95) where c = 0.13m/s is measured (Figure 12).

It is not unlikely that the retrogression velocity increases with grain size and increases with length scale. That the values found in the medium scale tests, with the exception of T95, are nearly equal to those in the large scale tests is due to the combination of both effects: larger grain size is larger (D_{50}=0.200mm versus D_{50}=0.145mm) and smaller length scale.

The influence of grain size may have to do with the process of dislodging: the larger the grain size, the quicker the dislodging.

The influence of length scale may be related to the value of Δz. The larger Δz, the higher the mean drop of the dislodged grains and the consequent higher flow velocity of these grains. The higher velocity and the larger sand discharge cause more shear load to the not yet dislodged grains (section 6.4.2), which causes an increase in dislodging speed. A higher flow velocity of the flowing sand grains yields a more than proportional increase in sand discharge if the thickness of the sand flow layer is proportional to Δz. Such increase goes along with a higher retrogression velocity.

7.7 Mean sand discharge s at x_0

The mean sand discharge, $s(x_0) = V.(1-n).\rho_s/T_{RGR}$ is presented in Figure 15. The discharge is roughly proportional to the thickness of the liquefied zone, which means that the discharge in the large scale tests is approximately 5 to 10 times as large as those in the medium scale tests. Some influence of grain size appears to be present as well: the larger the grain size, the larger the discharge.

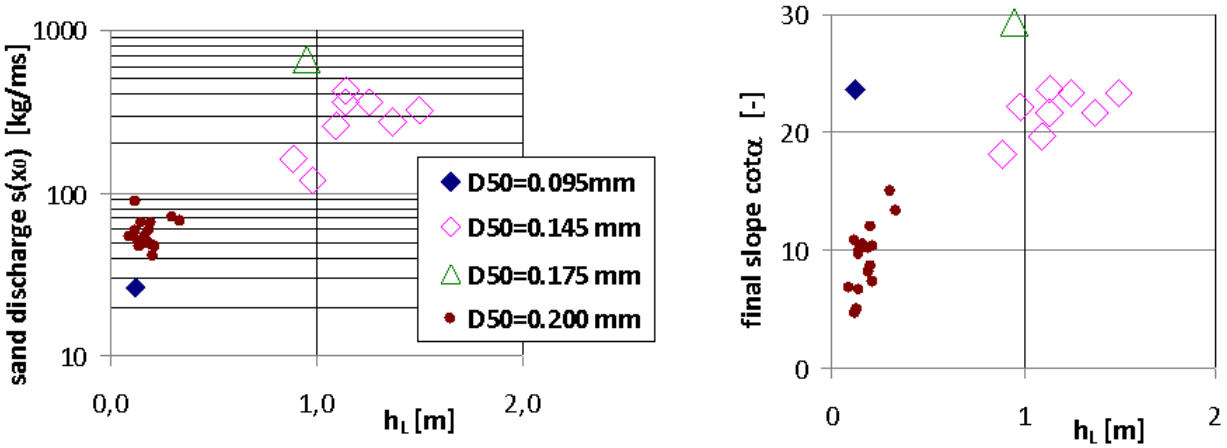

Figure 15 Sand discharge and final slope as function of liquefied height and grain size

The sand discharge is expected to be proportional to the product of the surface drop Δz, and the retrogression velocity c. The observed proportionality of s with the thickness of the liquefied zone h_L follows directly from the observed more or less constant values of $\Delta z/h_L$ and c. If it is correct that the observed constant value of c is due to a combination of the influences of length scale and grain size, then we may assume that the sand discharge s is more than proportional with the length scale if the grain size does not vary and that the sand discharge s increases with grain size.

7.8 Regression distance (x_0–x_{RGR})

The retrogression in one large scale test (OS7 with exceptional h=1m) and nearly all medium scale tests stopped before the end of the area of the fluidisation device. Most likely the slope α became so gentle that the sand, dislodged in the sand wave, could not flow away any more, even though excess pore pressures continued over a large part of the slope. The relative retrogression distance $(x_0–x_{RGR})/h_L$ varied between 12 and 31, with one remarkable exception: a value of 81 found for T95, the single test with very fine sand performed in the medium scale flume.

In the other large scale tests (all with h=2m) and in two of the medium scale tests (T28 and T31), retrogression stopped because the sand wave reached the end of the very loosely packed sand body. The relative retrogression distance in those tests varied between 15 and 28, which is not significantly different from the values in the other tests.

No significant influence of length scale is observed. Test T95 seems to indicate an increase in $(x_0–x_{RGR})/h_L$ with decreasing grain size. However, this is not confirmed by the other tests.

7.9 Final sand surface slope α

Length scale and grain size seem to have a significant influence on the final slope, as illustrated in Figure 15. The larger the liquefied height the more gentle the final slope. The influence of grain size is less clear, as just two tests with deviating grain sizes are available OS10 and T95. Comparison of OS10 with the other large scale tests suggests a more gentle slope with larger grain size. Comparison of T95 with the other medium scale tests strongly suggests the opposite.

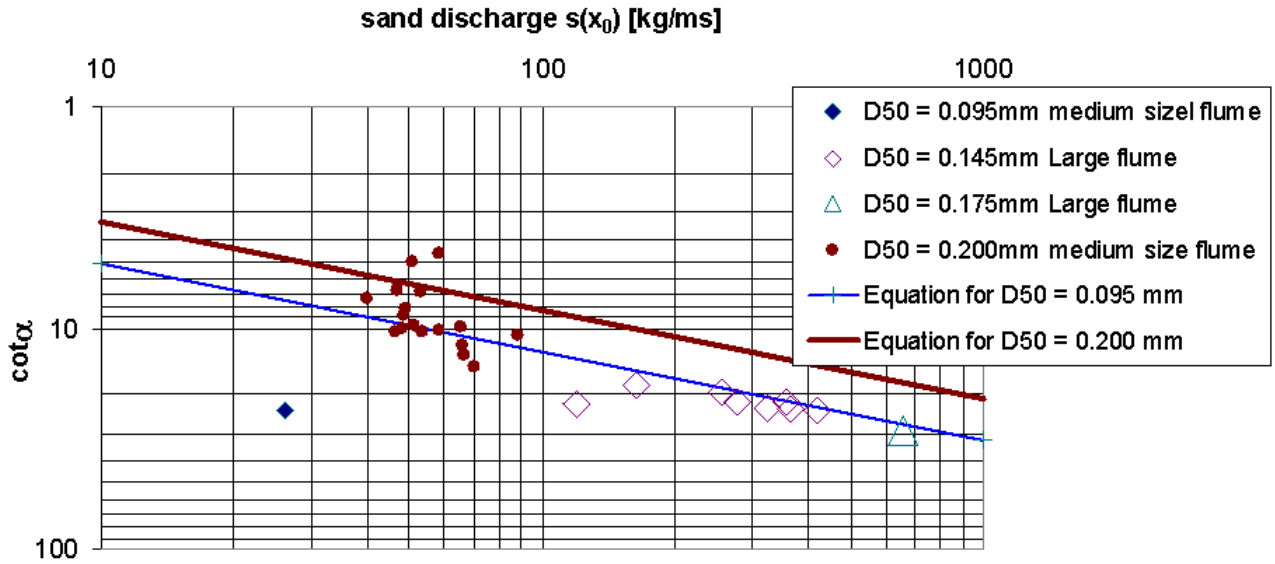

Figure 16 Final slope as a function of sand discharge in all tests resulting in flow slides

The final sand surface slope α is probably strongly related to the slope in the middle zone at the end of the retrogression period. The slopes are not exactly equal, but do not differ much. An equilibrium sand flow is expected in the middle zone (6.4.3). An empirical relationship between under water sand flow and equilibrium

slope is derived by (Mastbergen et al 1988, eq. 10): $\cot\alpha=0.5s^{0.4}/D_{50}^{0.6}$, if s expressed in kg/ms and D in mm. This equation is shown in Figure 16 for the grain diameters D_{50} = 0.095mm and D_{50} = 0.200mm, together with the results of all the tests resulting in flow slides, reported here. The presented values of $\cot\alpha$ refer to the final mean slope angles, which are not exactly equal to the slope angles present in the second zone during retrogression, but the differences are not very large. The agreement between observations and equations is fairly good, although the equations underestimate the influence of grain size. This agreement surprises, because the type of sand flow for which this relationship is derived is not a laminar flow, but a "turbulent hyperconcentrated density" flow as discussed in (Winterwerp et al 1990).

8 CONCLUSIONS

A. The experiments produce much information about a liquefaction flow slide in an under water sand body with a horizontal surface and a steep slope as initial boundaries. Further research is needed to find out if a similar flow slide may occur in a layer of loosely packed sand in a slope in response to a small instability. If so, then the quantity of soil material that flows down increases significantly. This may seriously increase the danger of a massive slope failure.
B. Such a slide differs significantly from a shear failure by the much larger distance of retrogression, the gentleness of the final slope (factor 10 or more). It differs from the retrogression of a breach in dilative sand by the much higher retrogression velocity (order factor 100) and by the fact that it does not require such a large initial instability as required for a breach failure.
C. Such a slide consists of the following processes:
    - Sudden liquefaction of the sand close to the slope
    - Flow down of sand grains from the top of the liquefied sand, resulting in a retrogressing negative sand wave
    - Liquefaction of sand at greater distance from the slope at the moment the sand wave passes
    - Flow down of sand grains also from the top of the newly liquefied sand, resulting in continued retrogression of the sand wave.
D. The physical background of the origin of liquefaction and the development of liquefaction in a column of sand are well known. The physical processes responsible for the dislodgement of grains from the surface and the flow of grains along the sloping surface, are not yet completely clear.
E. The most important conditions for a retrogressive liquefaction flow slide to occur are:
    - Very low relative density of the sand ($I_D < 0.2$ or $\psi > +0.10 \pm 0.05$)
    - An initial instability at the slope (a small one is sufficient)
    - Such a slope geometry that liquefied and dislodged sand has room to flow away
F. Retrogression may stop by two alternative mechanisms:
    - A pocket of more densely packed sand blocks the retrogression of liquefaction
    - The slope resulting after retrogression becomes too gentle to have all the dislodged sand grains flow away.

    The hypothetical possibility of retrogression stopping when the liquefaction ends is not observed.
G. Length scale and grain size seem to have the following effects at this type of flow slides:
    - Minimum layer thickness of approximately 0.3m to 0.5m required for flow slide to occur. Increase in liquefied height with layer thickness
    - Front slope slightly more gentle with larger liquefied height and larger grain size
    - Retrogression velocity slightly increases with liquefied height and grain size (tendency not clear)
    - Mean sand discharge increases more than proportional with liquefied height and increases with grain size
    - Final slope more gentle with increasing sand discharge and steeper with larger grain size.

LIST OF SYMBOLS

c	retrogression velocity [m/s]
c_v	consolidation coefficient for unloading [m^2/s]
D_{50}	median sand grain diameter [m]
e	void ratio [-]
e_c	void ratio of critical state line [-]
$e_{CRIT,DRY}$	dry critical void ratio[-]
$e_{CRIT,WET}$	wet critical void ratio [-]
e_{MAX}	maximum void ratio [-]
e_{MIN}	minimum void ratio [-]
G	Shear modulus for unloading [kPa]
h	height of original sand body (above fluidisation device) [m]
h_L	maximum thickness of liquefied zone, defined as $h_L = u_{MAX}/[(1-n)(\rho_s-\rho_w)g]$ [m]
I_D	density index $I_D = (e_{MAX} - e)/(e_{MAX} - e_{MIN})$ [-]
K	bulk modulus for unloading [kPa]
k	permeability [m/s]
$n=e/(1+e)$	porosity [-]
q_s	sand discharge expressed in volume including pores [m^2/s]
s	sand discharge expressed in mass [kg/ms]; $s(x_0) = V.(1-n).\rho_s/T_{RGR}$
t	time after initiation of instability [s]
$t(u_{MAX})$	time after the start of the process, as caused by lifting of the gate or otherwise, that u_{MAX} occurs [s]
T_{RGR}	retrogression period [s]
T_U	duration of excess pore pressure anywhere [s]
u	pore pressure in excess of hydrostatic pressure ("excess pore pressure") [kPa]
u_{MAX}	maximum value of u, i.e. highest value in time and place of the excess pore pressure at a distance of at least h from the original slope; remark: the values very close to the original slope are not representative for the process of retrogression of sand wave and liquefaction [kPa]
V	displaced volume of sand (including voids) per unit width [m^2]
x	horizontal distance [m]
x_0	x-value half way the original slope [m]
x_{RGR}	value of x to which sand wave retrogresses; $x_0 - x_{RGR}$ = retrogression distance [m]
x_{TOE}	value of x of toe of final slope; $x_{TOE} - x_0$ = flow distance [m]
z	height of sand surface above bottom of flume [m]
Δz	height loss, i.e. drop of sand surface of final surface observed at $x = (x_0+x_{RGR})/2$ [m]
dz/dt	height loss velocity at passing of sand wave observed at $x_0 - x = 12$m [m/s]
α	final slope angle, defined as: $\cot\alpha = (x_{TOE} + \|x_{RGR}\|)/(h+$height fluidisation device$)$
β	front slope angle of sand wave (Figure 9)
λ_{10}	slope of critical state line if stress is presented on decimal logarithmic scale
ρ_s	density of sand grains [kg/m^3]
ρ_w	density of water [kg/m^3]
σ_c	consolidation stress [kPa]
ψ	state parameter [-]

REFERENCES

Bagnold, R.A. (1954). Experiments on a gravity-free disperion of large solid spheres in a Newtonian fluid under shear. *Proc. Royal Society*. London, Vol. A 225, pp 49-63

Bezuijen, A. and Mastbergen, D.R. (1988). On the construction of sand fill dams – Part 2: Soil mechanical aspects. *Modelling Soil-Water-Structure Interactions, (eds. Kolkman et al)*, Balkema, Rotterdam, pp 363-371

De Groot, M.B. and Mastbergen, D.R. (2006). Scour hole slope instability in sandy soils. *Proc. 3rd Int. Conf. Scour and Erosion*. CURNET, Gouda, The Netherlands, pp 126-127

De Jager, R.R., Mathijssen, F.A.J.M., Molenkamp, F. and Nooy van der Kolff, A.H. (2008). Static liquefaction analysis using simplified modified state parameter approach for dredged sludge depot Hollandsch Diep. *12th Int. Conf. Int. Ass. for Computer Methods andAdvances in Geomechanics (IACMAG)* 1-6 October, Goa, India, 9 pages.

Jefferies, Mike and Been, Ken (2006). *Soil liquefaction. A critical state approach.* Taylor & Francis, London

Koppejan, A.W., Van Wamelen, B.M. and Weinberg, L.J.H. (1948). Coastal flow slides in the Dutch province of Zeeland. *Proc. 2nd Int. Conf. Soil Mech. & Foundation Eng.,*Rotterdam, Vol V, Section IV c 13, pp 89 - 96

Kramer, S.L. and Seed, H.B. (1988). Initiation of Soil Liquefaction Under Static Loading Conditions. *Journal of Geotechnical Engineering, Vol. 114, No.4*, American Society of Civil Engineers, pp 412-430

Kroezen M., Vellinga P., Lindenberg J. and Burger A M (1982). Geotechnical and hydraulic aspects with regard to seabed and slope stability. *Proc. 2nd Canadian Conf. Marine Geot. Eng. Halifax, NS, Canada* OR *Delft Hydraulics publication no. 272*, 13 pp

Lindenberg, J and Koning, H.L. (1981). Critical density of sand. *Geotechnique*, 31, No 2, 231-245

Mastbergen, D.R., Winterwerp, J.C. and Bezuijen, A. (1988). On the construction of sand fill dams – Part 1: Hydraulic aspects. *Modelling Soil-Water-Structure Interactions,* (Kolkman et al, eds), Balkema, Rotterdam, pp 353-362

Mastbergen, D.R. and Van den Berg, J.H. (2003). Breaching in fine sands and the generation of sustained turbidity currents in submarine canyons. *Sedimentology, Nr 50*, pp 635-637.

Silvis, F. and De Groot, M.B. (1995). Flow slides in the Netherlands: experience and engineering practice. *Canadian Geotechnical Journal 32*, pp 1086 - 1092

Van den Berg, H.J. (1987). In situ Testing of Soil. *Ground Engineer's Reference Book* (F.G. Bell ed), Butterworths, London, Section 25.6.4

Van Rhee, C. and Bezuijen, A. (1998). The breaching of sand investigated in large-scale model tests. *Proc. Int. Conf. Coastal Engineering (ASCE), Volume 3*, pp 2509-2519.

Winterwerp, J.C., De Groot, M.B., Mastbergen, D.R. and Verwoert, H.. (1990), Hyperconcentrated sand-water mixture flows over flat bed, *Journal of Hydraulic Engineering, Vol. 116, No. 1*, American Society of Civil Engineers, pp 36-54.